

Heavily Damped Motion of One-Dimensional Bose Gases in an Optical Lattice

Ippei Danshita¹ and Charles W. Clark²

¹*Department of Physics, Faculty of Science, Tokyo University of Science, Shinjuku-ku, Tokyo 162-8601, Japan*

²*Joint Quantum Institute, National Institute of Standards and Technology
and University of Maryland, Gaithersburg, Maryland 20899, USA*

(Dated: February 2, 2022)

We study the dynamics of strongly correlated one-dimensional Bose gases in a combined harmonic and optical lattice potential subjected to sudden displacement of the confining potential. Using the time-evolving block decimation method, we perform a first-principles quantum many-body simulation of the experiment of Fertig *et al.* [Phys. Rev. Lett. **94**, 120403 (2005)] across different values of the lattice depth ranging from the superfluid to the Mott insulator regimes. We find good quantitative agreement with this experiment: the damping of the dipole oscillations is significant even for shallow lattices, and the motion becomes overdamped with increasing lattice depth as observed. We show that the transition to overdamping is attributed to the decay of superfluid flow accelerated by quantum fluctuations, which occurs well before the emergence of Mott insulator domains.

PACS numbers: 03.75.Hh, 03.75.Lm, 05.30.Jp

Systems of ultracold bosonic atoms provide new opportunities to study many-body quantum physics in low dimensions, where thermal and quantum phase fluctuations play a crucial role. The unprecedented degree of controllability attainable in cold atom experiments has led to demonstrations of striking phenomena specific to low-dimensional systems, such as the purely one-dimensional (1D) Tonks-Girardeau gases [1, 2, 3] and the Kosterlitz-Thouless transition of 2D Bose gases [4, 5].

An array of 1D tubes of Bose gases can be created by imposing a strong transverse 2D optical lattice on a Bose condensed gas trapped in a parabolic potential. In recent experiments of this type, transport of 1D Bose gases has been investigated in the presence of another lattice potential along the 1D axis by displacing suddenly the parabolic potential [6, 7], and by using a moving optical lattice [8]. Strong inhibition of transport with increasing lattice depth has been observed in these cases. While 1D transport has also been studied in condensed matter systems, such as liquid ⁴He absorbed in nanopores [9] and superconducting nanowires [10], the flexible variability of optical lattice parameters allows for more detailed study in ultracold atomic gases. Moreover, the long relaxation time resulting from the diluteness of atomic gases offers the prospect of exploring dynamical properties of the transport over a wide range of conditions.

Fertig *et al.* [7] induced dipole oscillations of 1D Bose gases for different values of the axial lattice depth. They observed significant damping even for shallow lattices, and found a transition from underdamping to overdamping with increasing lattice depth. Due to strong quantum fluctuations, mean-field theories fail even qualitatively to describe the transport properties of 1D Bose gases, and recent theoretical analyses of this system have applied approaches beyond the mean-field approximation [11, 12, 13, 14, 15]. Good agreement with the experiment was obtained separately for the cases of shallow lattices, using a truncated Wigner approximation [12],

and for deep lattices, using an extended fermionization method [15]. However, so far the intermediate transition region remains poorly understood because the approaches used in the previous work are no longer valid there.

In this Letter, we present a direct simulation of this experiment from the shallow-lattice superfluid (SF) to the deep-lattice Mott insulator (MI) regimes, and we identify the specific physical mechanism governing the transition region. To properly include the effects of quantum fluctuations, we use the time-evolving block decimation (TEBD) method, which provides precise ground states and real-time evolution of 1D quantum lattice systems [16]. We show that the transition to overdamping is a manifestation of the decay of superfluid flow accelerated by strong quantum fluctuations, rather than that of the emergence of the MI domains.

We begin with the Bose-Hubbard model [17],

$$H = -J \sum_j (\hat{b}_j^\dagger \hat{b}_{j+1} + \text{h.c.}) + \frac{U}{2} \sum_j \hat{n}_j (\hat{n}_j - 1) + \Omega \sum_j (j + X_c/d)^2 \hat{n}_j, \quad (1)$$

where \hat{b}_j^\dagger creates a boson on the j -th site, and \hat{n}_j is the number operator. The parameters J , U , and Ω are related to independently-measurable experimental quantities. The hopping energy, J , is expressed as $J = A (V_0/E_R)^B \exp(-C\sqrt{V_0/E_R}) E_R$, where $A = 1.397$, $B = 1.051$, and $C = 2.121$ [14]. V_0 is the axial lattice depth and $E_R = \hbar^2/(8md^2)$ is the recoil energy, where m is the atomic mass and d is the lattice spacing. The onsite interaction, U , is given by $U = 2(a_s/d)\sqrt{2\pi V_\perp/E_R} (V_0/E_R)^{1/4} E_R$, where a_s is the s -wave scattering length and V_\perp is the depth of the lattice in the transverse directions. The parabolic trap is centered at $-X_c$, and its curvature, Ω , is given by

$\Omega = m\omega_T^2 d^2/2$, where ω_T is the frequency of the external harmonic potential. In the experiment, $X_c = 0$ for $t < 0$, and it is suddenly displaced to $X_c = x_0$ at $t = 0$ to cause dipole motions of the Bose gas. Note that the Bose-Hubbard model is quantitatively valid only when the lattice depth is sufficiently large as $V_0 \gtrsim 2E_R$ [14].

To compare our calculations with the experiment of Fertig *et al.* [7], we use $a_s = 5.31$ nm, $d = 405$ nm, $V_\perp = 30E_R$, and $\omega_T = 2\pi \times 60$ Hz. In the experiment, the atoms were confined in a 2D array of decoupled tight 1D tubes and an additional periodic potential was added along the direction of the tubes. We focus on the central tube with the number of atoms $N = 81$.

To treat the dynamics at zero temperature associated with Eq. (1), we use the TEBD method, which allows us to compute accurately the evolution of many-body wave functions of 1D quantum lattice systems [16]. We choose the maximum number of atoms per site $n_{\max} = 5$ and retain up to $\chi = 200$ states in the adaptively selected Hilbert space (for the definition of χ and a detailed convergence analysis, see Ref. [18]). Setting $X_c = 0$, we first calculate the ground states of Eq. (1) via propagation in imaginary time. At $t = 0$ the trap center X_c is suddenly displaced by the distance x_0 to cause dipole motions, and we simulate the dynamics of the system via propagation in real time. In the experiment, the initial displacement was fixed to be $x_0 \simeq 8d$ and V_0/E_R was changed in the range of $0 \leq V_0/E_R \leq 9$ [7]. Here we also study the dependence of the damping on x_0 , so as to reveal the effects of the decay of superfluid flow.

In Figs. 1(a)-(d), we show the local densities $n_j \equiv \langle \hat{n}_j \rangle$, and their fluctuations, $\sigma_j \equiv (\langle \hat{n}_j^2 \rangle - n_j^2)^{1/2}$, of the ground states of the system for lattice depths $V_0/E_R = 2, 3, 4$, and 8. When $V_0 = 2E_R$, the density profile is smooth, with the reflected parabolic shape of the confining potential that is characteristic of SF phases. As V_0/E_R is increased, the density profile around $n_j = 1$ becomes distorted and the fluctuation σ_j starts to take minima at $n_j = 1$ as seen in Fig. 1(c), precluding the emergence of the incompressible MI domains with unit filling. When $V_0 = 8E_R$ (Fig. 1(d)), the unit-filling MI plateaus are formed and its presence is convinced by the fact that the value of σ_j in the plateaus coincides with the value of the fluctuation in the homogeneous system for the unit filling and the same value of J/U [19].

In Figs. 1(e)-(h), we show the c.m. position $x_{\text{cm}} = N^{-1}d \sum_j j \langle \hat{n}_j \rangle$ as a function of time for $x_0 = d$ and different values of V_0/E_R . Note that this displacement amplitude is substantially smaller than that employed in the experiment of Ref. [7]; we return to the specific experimental simulation below, after identifying an important point of physics that is seen most clearly in the small-displacement regime. The c.m. velocity $\dot{x}_{\text{cm}}(t)$ for $V_0 = 3E_R$ is also shown by a dotted line in Fig. 1(f). When $V_0 = 2E_R$, the oscillation is hardly damped; this means that the Bose gas behaves as a superfluid as long

as its velocity is small. As V_0/E_R is increased, noticeable damping is already seen at $V_0 = 3E_R$. At $V_0 = 4E_R$, the oscillation is drastically damped while it remains in the underdamped regime according to the definition of underdamping mentioned below. This means that the suppression of fluctuations at $n_j = 1$ results in significant reduction of the mobility of the Bose gas even before the formation of the MI domains. When the lattice is very deep ($V_0 = 8E_R$), the motion is overdamped.

Following the method used by Ref. [7], we model the c.m. motion of the Bose gas in our results as a damped harmonic oscillator, $m^* \ddot{x} = -b\dot{x} - kx$, to extract a damping rate b/b_0 as a function of V_0/E_R and x_0/d , where m^* is the effective mass, $k \equiv m\omega_T^2$, and $b_0 \equiv 2m\omega_T$ [20]. We regard the c.m. motion as underdamped if the c.m. position oscillates across the trap center, $x = -x_0$. In this

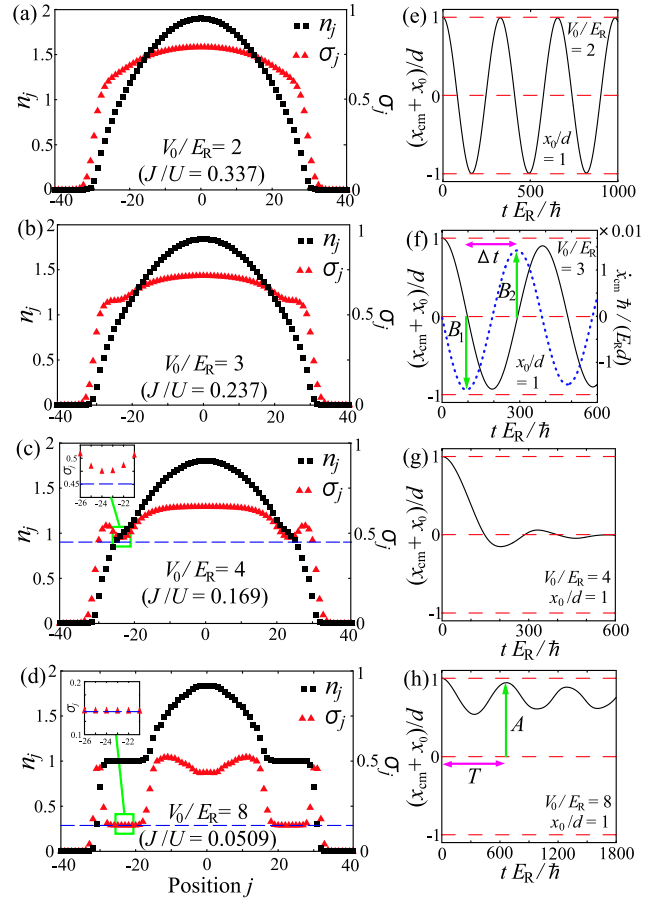


FIG. 1: (color online) Results at four values of V_0/E_R : 2 (a) and (e), 3 (b) and (f), 4 (c) and (g), and 8 (d) and (h). In the left four figures, we show the local densities $n_j \equiv \langle \hat{n}_j \rangle$ (squares) and fluctuations σ_j (triangles) of the ground states. The dashed lines in (c) and (d) represent the fluctuations for the unit-filling in the homogeneous Bose-Hubbard system, calculated with the use of the infinite-size version of the TEBD [27]. In the right four figures, we show the time evolution of the c.m. position $x_{\text{cm}}(t)$ for a small displacement $x_0 = d$. In (f), $\dot{x}_{\text{cm}}(t)$ is also plotted by a dotted line.

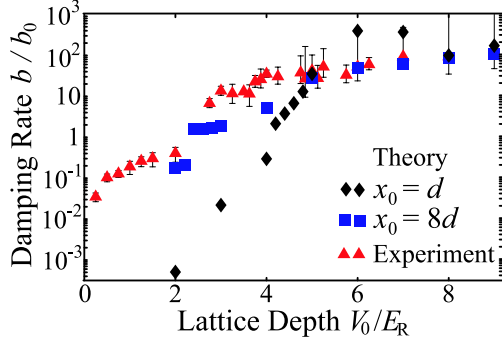


FIG. 2: (color online) Damping rate b/b_0 versus V_0/E_R for $x_0 = d$ (diamonds) and $x_0 = 8d$ (squares). The triangles are the experimental results of Ref. [7].

definition, for instance, the c.m. motions for $V_0/E_R = 2, 3$, and 4 and $x_0 = d$ shown in Figs. 1(e)-(g) are underdamped. On the other hand, the c.m. motion is regarded as overdamped if the first minimum of the c.m. position does not reach the trap center as seen in Fig. 1(h). To obtain the damping rate, we use the minimum and maximum values of x_{cm} and \dot{x}_{cm} within the first oscillation. For underdamped motion, where $b < b_0$, the damping rate is given by $b = 2m^* \ln(B_1/B_2)/\Delta t$, where B_1 and B_2 are the absolute values of \dot{x}_{cm} at the first and second extrema, respectively, and Δt is the time interval between the two extrema as indicated in Fig. 1(f). For overdamped motion, where $b > b_0$, the damping rate is determined by solving $\bar{x}_{\text{cm}}(T) = A$ for b , where A and T are the values of x_{cm} and t at the first maximum (see Fig. 1(h)), and $\bar{x}_{\text{cm}}(t)$ is the solution to the overdamped harmonic oscillator equation.

In Fig. 2, we show the damping rates for $x_0 = d$ and $8d$ as a function of V_0/E_R , together with the experimental data of Ref. [7] where $x_0 \simeq 8d$. In the experiment, the motion becomes overdamped with increasing the lattice depth, starting between $V_0/E_R = 2$ and 3. Our TEBD simulations for $x_0 = 8d$ are in good agreement with the experimental results; the onset of the overdamping lies between $V_0/E_R = 2.2$ and 2.4, where the MI domains are not present. This reveals that the transition to overdamping observed in the experiment is not due to the emergence of the MI domains. Notice that although the damping rate b/b_0 exhibits a jump at the transition point, the actual mobility of the Bose gas is gradually reduced and this jump is only superficial [18].

The mechanism of damping in the transition region is suggested in Fig. 3, which shows the maximum c.m. velocities $\bar{v}_{\text{cm}}^{\text{max}}$ and the damping rates for different values of V_0/E_R as functions of x_0/d . For a given value of the lattice depth, the damping becomes more significant as $\bar{v}_{\text{cm}}^{\text{max}}$ increases, and the motion eventually changes from underdamping to overdamping. This behavior is analogous to the breakdown of superfluid flow observed in the experiment of Ref. [8] by using a moving optical lattice, where

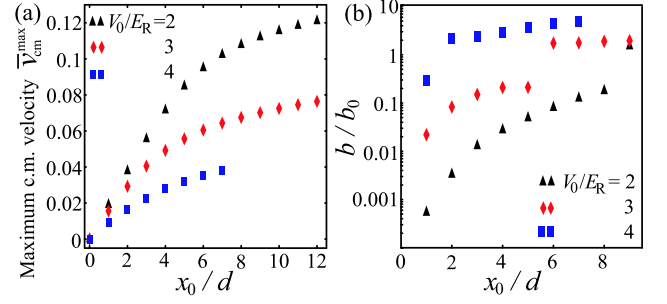


FIG. 3: (color online) Maximum c.m. velocities $\bar{v}_{\text{cm}}^{\text{max}} \equiv |B_1|$ (a) and damping rates b/b_0 (b) for $V_0/E_R = 2$ (triangles), 3 (diamonds), and 4 (squares) as functions of x_0/d .

a transition from superfluid flow to dissipative flow is induced as the lattice velocity is increased [21]. Hence, this strong velocity dependence of the damping rate implies that the transition to overdamping can be attributed to the breakdown of superfluid flow.

To confirm this suggestion, we show the time evolution of the non-condensate fraction $\bar{n}_{\text{non}}(t) \equiv (N - N_c)/N$ in Fig. 4(a), where the number of the condensate bosons N_c is defined as the largest eigenvalue of the one-body density matrix $\langle \hat{b}_j^\dagger \hat{b}_l \rangle$ [22]. Notice that despite the one-dimensionality of our system, the condensate fraction N_c/N of the superfluid ground states is of order one because our system is finite. Since as a consequence of the breakdown of superfluid flow, excitations kick particles out of the condensate increasing the non-condensate fraction, the breakdown can be identified by growth of the non-condensate fraction in time as done in the experiment of Ref. [8]. In Fig. 4(a), for small displacement ($x_0 = 2d$) \bar{n}_{non} hardly changes as t increases; accordingly the superfluid flow is stable. The growth of \bar{n}_{non} in time becomes more prominent as x_0/d increases, namely, as the damping becomes more significant. This means that the c.m. motion is damped by the transference of kinetic energy into non-condensate excitations accompanied by the breakdown of superfluid flow. In Fig. 4(b), one sees that the growth rate $d\bar{n}_{\text{non}}/dt$ takes its maximum value immediately after the c.m. velocity peaks. In Fig. 5, we show the maximum value of the growth rate $d\bar{n}_{\text{non}}/dt|_{\text{max}}$ for different values of the lattice depth as a function of $\bar{v}_{\text{cm}}^{\text{max}}$. The maximum growth rate is increased as either $\bar{v}_{\text{cm}}^{\text{max}}$ or V_0/E_R is increased. When $x_0 = 8d$ as chosen in the experiment [7], the breakdown of superfluid flow is so severe that it leads to significant damping already in the underdamped regime. As V_0/E_R is increased, superfluid flow breaks down even more severely and the c.m. motion gradually changes to overdamping. Therefore, the transition to overdamping observed in the experiment is due to the breakdown of superfluid flow. One can experimentally corroborate this interpretation by measuring the non-condensate fraction and specifying its growth associated with the significant damping be-

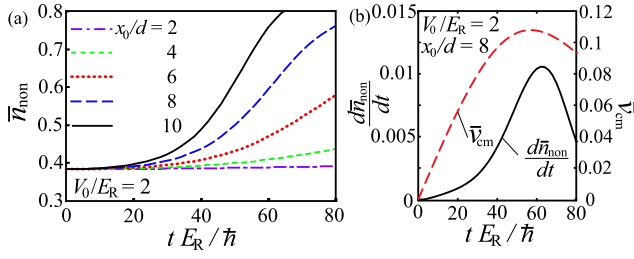


FIG. 4: (color online) (a) Time evolution of the non-condensate fraction $\bar{n}_{\text{non}}(t)$ at $V_0 = 2E_R$ for different values of the displacement. (b) Time evolution of $d\bar{n}_{\text{non}}/dt$ (solid line) and \bar{v}_{cm} (dashed line) for $V_0 = 2E_R$ and $x_0 = 8d$.

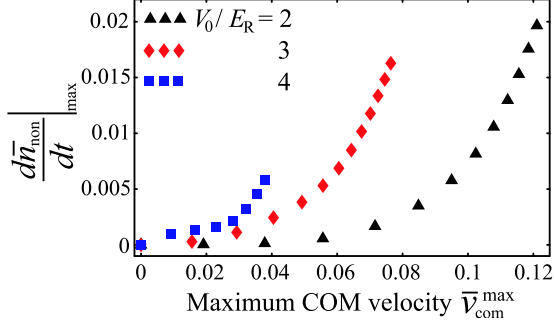


FIG. 5: (color online) Maximum growth rates $d\bar{n}_{\text{non}}/dt|_{\text{max}}$ of the non-condensate fraction for $V_0/E_R = 2$ (triangles), 3 (diamonds), and 4 (squares) as functions of $\bar{v}_{\text{cm}}^{\text{max}}$.

cause the non-condensate fraction is one of the typical observables in experiments [8].

We now discuss the effects of quantum fluctuations on the breakdown of superfluid flow. As seen in Fig. 5, in the 1D Bose gases $d\bar{n}_{\text{non}}/dt|_{\text{max}}$ grows gradually with increasing $\bar{v}_{\text{cm}}^{\text{max}}$ in contrast to 3D Bose condensates, where a transition from superfluid to dissipative flow occurs very sharply [8]. Moreover, the superfluid flow breaks down significantly even at much lower velocity than the critical velocity v_{cr} for the dynamical instability predicted by mean-field theories [23] (for instance, $v_{\text{cr}} \simeq 0.288E_R d/\hbar$ when $V_0 = 2E_R$ [24]). The smearing and reduction of the critical velocity stem from strong quantum fluctuations specific to the 1D systems [8], which allow for the decay of the supercurrent through macroscopic quantum tunneling [26]. Thus, the quantum fluctuations accelerate the decay of superfluid flow, leading to the heavily damped motion observed in the experiment.

In conclusion, we have studied damped dipole oscillations of one-dimensional Bose gases in an optical lattice by using the time-evolving block decimation method. We have shown that the center of mass motion changes from

underdamping to overdamping as observed in the experiment [7] because strong quantum fluctuations accelerate the decay of superfluid flow, which is characterized by prominent growth of the non-condensate fraction in time.

The authors thank Trey Porto for helpful discussions and for providing the experimental data. I. D. acknowledges discussions with S. Konabe, S. Tsuchiya, and K. Kamide and support from a Grant-in-Aid from JSPS. This work was partially supported by the NSF under Physics Frontiers Center award PHY-0822671.

-
- [1] B. Paredes *et al.*, *Nature* **429**, 277 (2004).
 - [2] T. Kinoshita *et al.*, *Science* **305**, 1125 (2004).
 - [3] T. Kinoshita *et al.*, *Nature* **440**, 900 (2006).
 - [4] Z. Hadzibabic *et al.*, *Nature* **441**, 1118 (2006).
 - [5] P. Cladé *et al.*, arXiv:0805.3519 (2008).
 - [6] T. Stöferle *et al.*, *Phys. Rev. Lett.* **92**, 130403 (2004).
 - [7] C. D. Fertig *et al.*, *Phys. Rev. Lett.* **94**, 120403 (2005).
 - [8] J. Mun *et al.*, *Phys. Rev. Lett.* **99**, 150604 (2007).
 - [9] R. Toda *et al.*, *Phys. Rev. Lett.* **99**, 255301 (2007).
 - [10] N. Giordano, *Phys. Rev. Lett.* **61**, 2137 (1988); A. Bezyadin *et al.*, *Nature* **404**, 971 (2000); F. Altomare *et al.*, *Phys. Rev. Lett.* **97**, 017001 (2006).
 - [11] A. Polkovnikov *et al.*, *Phys. Rev. Lett.* **93**, 070401 (2004).
 - [12] J. Ruostekoski *et al.*, *Phys. Rev. Lett.* **95**, 110403 (2005).
 - [13] M. Rigol *et al.*, *Phys. Rev. Lett.* **95**, 110402 (2005).
 - [14] A. M. Rey *et al.*, *Phys. Rev. A* **72**, 033616 (2005).
 - [15] G. Pupillo *et al.*, *New J. Phys.* **8**, 161 (2006).
 - [16] G. Vidal, *Phys. Rev. Lett.* **93**, 040502 (2004).
 - [17] M. P. A. Fisher *et al.*, *Phys. Rev. B* **40**, 546 (1989).
 - [18] See EPAPS Document No. E-PRLTAO-102-035906 for supplementary material. For more information on EPAPS, see <http://www.aip.org/pubservs/epaps.html>.
 - [19] M. Rigol *et al.*, *Opt. Commun.* **243**, 33 (2004).
 - [20] As seen in Fig. 1(h), the motion in the overdamping region still oscillates and is different from an overdamped oscillator represented by a simple mechanical model. However, we model this motion as an overdamped oscillator to compare our results with the experiment [7].
 - [21] A widely used definition of superfluid flow is “flow without dissipation”, which we also use in this paper.
 - [22] O. Penrose and L. Onsager, *Phys. Rev.* **104**, 576 (1956).
 - [23] B. Wu and Q. Niu, *Phys. Rev. A* **64**, 061603(R) (2001); A. Smerzi *et al.*, *Phys. Rev. Lett.* **89**, 170402 (2002).
 - [24] Mean-field theories also predict the Landau instability characterized by excitations with negative energies [23]. However, it cannot destabilize superfluid flow at zero temperature [25], and is not relevant to our case.
 - [25] L. De Sarlo *et al.*, *Phys. Rev. A* **72**, 013603 (2005); S. Konabe *et al.*, *J. Phys. B* **39**, S101 (2006); K. Iigaya *et al.*, *Phys. Rev. A* **74**, 053611 (2006).
 - [26] A. Polkovnikov *et al.*, *Phys. Rev. A* **71**, 063613 (2005).
 - [27] G. Vidal, *Phys. Rev. Lett.* **98**, 070201 (2007).